Nat. Hazards Earth Syst. Sci. Discuss., https://doi.org/10.5194/nhess-2017-337
Manuscript under review for journal Nat. Hazards Earth Syst. Sci.
Discussion started: 10 October 2017
© Author(s) 2017. CC BY 4.0 License.

Natural Hazards and Earth System Sciences
Discussions

Quick Response Assessment of the Impact of an Extreme Storm Combining Aerial Drone and RTK GPS

Arthur C. Trembanis[1], Enrico Duo[2], Stephanie Dohner[1], Edoardo Grottoli[2], and Paolo Ciavola[2]

[1]School of Marine Science and Policy, University of Delaware
[2]Department of Physics and Earth Sciences, University of Ferrara

Correspondence to: Arthur C. Trembanis (E-mail: art@udel.edu Tel.: 1-302-831-2498)

Abstract. Developing and implementing a quick response post-storm survey protocol ~~has the potential~~ to improve impact assessments of coastal storms. Pre- and post-event surveys are essential to properly quantify the storm impacts on the coast. In this study, a combination of traditional RTK GPS and Unmanned Aerial Vehicle "drone" platform was utilized as part of a coordinated storm response workflow. The comprehensive approach employed in this pilot case study was conducted on the Emilia-Romagna coast (Italy), in the immediate aftermath of an extreme storm event that impacted the shoreline on the 5th-6th February 2015 called the "Saint Agatha Storm". The activities were supported by timing information on the approaching storm provided by the regional early warning system. We collected aerial photos from a commercial off-the-shelf drone immediately after the Saint Agatha Storm and generated both orthomosaic and digital elevation models utilizing structure-from-motion photogrammetry techniques. The drone-based survey approach allowed ~~us to quickly~~ survey an area of 0.25 km^2 within a 10-minute flight resulting in a ground sampling distance of 2.5 cm/pixel. Flooding and erosion impacts are analyzed and presented for the target study area. Limitations and possible applications for coastal management of the quick response post-storm surveying protocol are highlighted.

1 Introduction

Coastal flooding and erosion linked with extreme storm events shape coastlines, impact coastal infrastructure, and present hazards to ~~coastal inhabitants that can thus suffer their consequences~~. The most damaging events consist of a combination of extreme wave heights, storm surge, wind direction~~,~~ and tidal stage~~,~~ that interact with the morphology of the beach and adjacent infrastructures generating direct and indirect impacts (Van Dongeren et al., 2017; Viavattene et al., 2017). With expectations of increasing storm intensities and occurrence (Bason et al., 2007), coastal communities are in need of accurate field data to inform management and policy decisions (Casella et al., 2016). To ensure appropriate plans are enacted, precise and high-resolution field geomorphology measurements are required to understand storm effects on ~~the community~~ and to provide input for numerical modeling for future impact prediction purposes (Lee et al., 1998; Stone et al., 2004; Nicholls et al., 2007). Capturing the signature of a storm event requires a rapid quantitative mapping response to assess the impacts to the coastline after the storm, before either natural or human ~~induced recovery processes begin to~~ take place (Morton et al., 1993; Bush et

Nat. Hazards Earth Syst. Sci. Discuss., https://doi.org/10.5194/nhess-2017-337
Manuscript under review for journal Nat. Hazards Earth Syst. Sci.
Discussion started: 10 October 2017
© Author(s) 2017. CC BY 4.0 License.

Natural Hazards and Earth System Sciences
Discussions

al., 1999; Morton, 2002). ~~Notably, in~~ order to properly quantify these impacts, it is also desirable to collect recent pre-storm elevation data. In recent years, robotic platform methodologies for coastal mapping and extreme event impact assessment were proposed and tested~~,~~ beyond the traditional GPS, LIDAR~~,~~ and satellite remote sensing techniques, such as the use of unmanned vehicles for mapping the emerged beach (Mancini et al., 2013; Casella et al., 2016; Turner et al., 2016) and the submerged area (Trembanis et al., 2013).

~~The classic stadia rod and level beach surveying technique, while still functional, has been replaced by time and cost efficient~~ Real-Time Kinematic Geographical Positions Systems (RTK GPS) for ground-based surveys (Morton et al., 1993; Theuerkauf and Rodriguez, 2012). RTK GPS is the preferred method for any data collection requiring highly accurate (few centimeter) positioning measurements and is utilized in the coastal environment for temporal and spatial monitoring of many coastal morphologic features (Larson and Kraus, 1994; Benedet et al., 2007; Hansen and Barnard, 2010; Theuerkauf and Rodriguez 2012). With RTK GPS surveys, questions arise regarding the accuracy of beach morphology representation due to insufficient resolution when traditional profile spacings of more than 100 meters are used (Swales, 2002; Berstein et al, 2003; Pietro, et al., 2008; Theuerkauf and Rodriguez, 2012). Terrestrial laser scanners or total stations improve point density but require similar time and physical effort as RTK GPS, particularly when surveying large areas (Saye et al., 2005; Theuerkauf and Rodriguez, 2012; Lee et al., 2013). Improvements in remote sensing technology have increased point density through airborne lasers (LiDAR) and satellite imagery but the high costs of operations and infrequent surveys render these options impractical for local scales and rapid or frequent repeated surveys (Stockdon et al., 2002; Young and Ashford, 2006; Anderson and Gaston, 2013). Recent improvements in autonomous technology have made Unmanned Aerial Systems (UAS) a useful emerging tool in the survey world which accommodates local scales, rapid and frequent surveys, and can be economically feasible with accurate results for monitoring hydro-morphological changes in the coastal zone (Berni et al., 2009; Westoby et al., 2012; Casella et al., 2016; James et al., 2017).

Here we present a pilot case study of a quick response protocol for assessing storm impacts utilizing a combination of traditional on-ground RTK GPS surveys together with aerial imagery gathered by an Unmanned Aerial Vehicle (UAV or drone) for digital photogrammetry reconstruction further supported by qualitative data collection. The presence of an operational Early Warning System in the area is essential for the rapid response planning. This combination of technologies allows for a rapid and more holistic coverage of the field site. The presented results of the pilot test demonstrate that the approach can provide high-resolution data for capturing storm impacts. Furthermore, this integrated approach can provide detailed insights that can be applied at the local, property scale of stakeholders, as well as at regional and national levels for coastal management purposes.

Nat. Hazards Earth Syst. Sci. Discuss., https://doi.org/10.5194/nhess-2017-337
Manuscript under review for journal Nat. Hazards Earth Syst. Sci.
Discussion started: 10 October 2017
© Author(s) 2017. CC BY 4.0 License.

Natural Hazards and Earth System Sciences
Discussions

2 Study area

2.1 Regional settings

A stretch (~7 km) of the coastal area of the Ferrara province (Emilia-Romagna region), on the Italian side of the Northern Adriatic Sea (Fig. 1A, 1B), was surveyed ~~starting in the waning period of~~ an extreme storm event (hereafter called the Saint Agatha storm, see Section 3) that occurred on February 5-7th, 2015. ~~The survey continued for a week following the passage of the storm~~. The coastal landscape in Emilia-Romagna is generally comprised of low-lying sandy beaches with limited topographically elevated areas usually in the form of either relict beach ridges or artificial embankments (Armaroli et al., 2012). The shore is comprised of alternating spaces of natural areas with native dunes and intermixed with more prevalent urbanized areas with tourist facilities and coastal protection structures (i.e. groins and breakwaters). Through continued development and urbanization over the last 60 years as a result of grants to commercial beach concession operators, most of the shore is now occupied by tourist facilities, residential buildings, and bathing structures often replacing the ancient coastal dune ridges (Sytnik and Stecchi, 2014). Since the end of World War II, a sediment deficit has affected the littoral budget as a result of a decrease in sediment transport towards the shore by local rivers, mainly because of the human interventions on the rivers and their basins (Preciso et al., 2012) and the reforestation of the Apennines (Billi and Rinaldi, 1997). The exposure to coastal flooding is high, especially in the Ferrara and Ravenna provinces, ~~where some elevations are below Mean Sea Level (MSL),~~ (Perini et al., 2010), and several defense structures (groins, breakwaters, etc.) have been built along the coast in the hope that beach retreat would cease (Armaroli et al., 2012).This problem has been exacerbated over the last few decades by land subsidence, which has been caused mostly by groundwater and gas extraction activities (Teatini et al., 2005; Taramelli et al., 2015). The subsequent vulnerability of local beaches to storm events led to the development of an Early Warning System (EWS), in the framework of the EU FP7 MICORE project (www.micore.eu), with the objective ~~to predict~~ the imminent arrival of a storm as a tool to be used by civil protection agencies and local communities (Ciavola et al., 2011; Harley et al., 2012; Harley et al., 2016). The Emilia-Romagna EWS is operational and is run by executing a daily sequence of connected numerical models (COSMO, SWAN, ROMS, and XBeach), comprised of 22 cross-shore profiles, with the final output transformed into a format suitable for decision-makers and end-users (Harley et al., 2012). The EWS tool is based on storm impact indicators (Ciavola et al., 2011), focusing on water intrusion and the type of exposed assets, which are described as natural or urbanized beaches (Harley et al., 2016).

The wave climate for the region is characterized by low wave energy (mean Hs ≈ 0.4 m, Tp ≈ 4 s) with a semidiurnal microtidal regime (neap tidal range= 0.30 m; spring tidal range = 0.8 m). Storm waves with 1-year return period range up to 3.3 m (Armaroli et al., 2009) and storm surges with a 2-year return period are up to 0.6 m (Masina and Ciavola, 2011). These storm events can occur, particularly in the fall and winter months (October-March), which comprises the storm season. Storms are mainly characterized by ENE waves associated with Bora (NE) winds or by SE waves if caused by Scirocco (SE) winds. Storm surge events predominantly occur during SE (Scirocco) winds, which also coincide with the main SE–NW orientation of the

Nat. Hazards Earth Syst. Sci. Discuss., https://doi.org/10.5194/nhess-2017-337
Manuscript under review for journal Nat. Hazards Earth Syst. Sci.
Discussion started: 10 October 2017
© Author(s) 2017. CC BY 4.0 License.

Natural Hazards and Earth System Sciences
Discussions

Adriatic Sea. Bora storm waves are generally large and steep, whereas Scirocco waves are smaller but with a longer wave period. This is because the latter are generated over a longer fetch by winds of lower intensity (Harley et al., 2016).

Several methods for storm characterization have been developed and implemented in recent years for the Mediterranean coast. Mendoza et al., (2011) proposed a five-class intensity scale, defining a storm as an event in which the significant wave height exceeds 1.5m for at least 6 hours (Mendoza and Jiménez, 2006). Moving to a more local perspective, Armaroli et al., (2012) adopted the same physical definition of storm events for the northern Adriatic. Two storms were considered separated when the significant wave height decreases below the 1.5 m threshold for 3 or more consecutive hours. As a resulting of the combined analysis of the events and their impacts, Armaroli et al., (2012) classified a storm as "potentially damaging" when it exceeds the critical wave and total water level (TWL=surge+tide) threshold which are: Hs>=2m and TWL>=0.7m for urbanized beaches; Hs>=3.3m and TWL>=0.85m for natural beaches. The Saint Agatha storm was identified utilizing the nearest offshore buoy and tide gauge (Fig. 1C & 2) records for waves and water levels, and following the Armaroli et al., (2012) storm definition.

2.2 Case study site and target area

The case study site is the portion of coast between Porto Garibaldi and Lido di Spina and is characterized by highly developed, low-lying sandy beaches, with commercial concessions directly facing the sea. The width of the beach ranges from ~20m to ~150m. The predominant sediment transport (longshore drift) is directed northward. The southern jetty of Porto Garibaldi traps this sediment, resulting in widening of the beach of Lido degli Estensi and depleting the Porto Garibaldi beach. Erosion appears again in the southern part of Lido di Spina (Nordstrom et al., 2015), as it can be seen in Fig. 1D. The southernmost concession at Lido di Spina defines the southern boundary of the case study. In the whole area, the concessions can be affected by coastal storm impacts during extreme events (Nordstrom et al., 2015). The whole pilot case study is well known at regional level as coastal risk prone area (Perini et al., 2016; Armaroli and Duo, 2017). The target area of the analysis of this pilot study, is the southernmost portion of the beach at Lido degli Estensi (Fig. 1E) in the municipality of Comacchio, east of Ferrara and north of Ravenna.

~~**Figure 1. Field study site locations: A) Emilia-Romagna region; B) Coastal regional domain; C) Locations of the nearest tide gauge and wave buoy; D) Pilot case study site; E) Target area for data comparison.**~~

3 Storm event

During the period February 5-7th, 2015, an extreme storm hit the Emilia-Romagna coast and the whole of the northern Adriatic Sea, causing flooding of extensive portions of urban and natural areas. The storm occurred in the context of extreme regional weather conditions, which included heavy snow in the Apennines and rain in the alluvial plain of the Emilia-Romagna region (Arpa Emilia-Romagna, 2015; Perini et al., 2015a & b). ~~As anticipated, the authors will refer to the storm by the colloquial name of the Saint Agatha storm as it occurred during the feast of Saint Agatha~~. The storm started at night and lasted for ~~more than two days (~~51 h~~)~~, making it one of the longest duration storms in the record of the local wave buoy offshore of Cesenatico

Nat. Hazards Earth Syst. Sci. Discuss., https://doi.org/10.5194/nhess-2017-337
Manuscript under review for journal Nat. Hazards Earth Syst. Sci.
Discussion started: 10 October 2017
© Author(s) 2017. CC BY 4.0 License.

Natural Hazards and Earth System Sciences
Discussions

(Fig. 1C)~~, deployed~~ in May 2007. The maximum water level (surge + tide) of 1.20m was measured at 23:40 GMT on 5th February~~. However,~~ the maximum significant wave height (4.6m) was recorded 8 hours later~~,~~ on the morning of 6th February (Fig. 2). The wave direction was consistently from the ENE sector for the entire event duration. The recorded water level was provided by the tide gauge of ISPRA (Istituto Superiore per la Protezione e la Ricerca Ambientale) located in Porto Corsini, Ravenna (Fig. 1C). Wave data was recorded by the ARPA-ER (Agenzia Regionale per la Prevenzione e l'Ambiente dell'Emilia-Romagna) offshore wave buoy located at 10m depth, 5.5km offshore from the town of Cesenatico (Fig. 1C). According to the Mediterranean storm classification of Mendoza et al. (2011), the Saint Agatha storm ~~can be assigned to the~~ severity class IV ("Severe"). The storm severity was amplified by the combination of high waves, high water level, and intense rainfall that created combined problems to the local river discharge (Perini et al., 2015a & b). Furthermore, according to the classification of Armaroli et al., (2012), the Saint Agatha storm was expected to have a strong impact on the coast, exceeding the combined wave and water level hazard thresholds over a wide area (Fig. 2). Notably, the event was forecasted by the regional coastal EWS (Perini et al., 2015b). Thus, this extreme event storm provided a unique opportunity to operationalize and evaluate the effectiveness of a comprehensive rapid storm response protocol.

Severe damage to several concession properties and urban areas was recorded along the coast. A description of the impacts at regional level can be found in Perini et al. (2015a & b). As part of the quick response effort, our team was able ~~to visit~~ several locations~~,~~ in the Ferrara and Ravenna provinces~~, in the~~ two weeks ~~immediately following~~ the ~~event, with a focus on directly observing and quantifying the impacts of the event, where rapid human post-storm intervention did not occur. While in~~ the Ferrara province the impacts were mainly confined to the exposed beach, causing significant damage to the concessions (urbanized beaches), to the dune systems (natural areas) and smaller harbors (e.g. flooding of the Porto Canale in Porto Garibaldi)~~, in~~ the Ravenna province several coastal towns experienced extensive flooding of residential areas (e.g. Lido di Dante, Classe and Savio) mainly due the low elevation of the southern part of the regional coastal corridor (Perini et al., 2010). In this paper we present our analysis on the impacts at a local level in the Comacchio municipality (i.e. the target area in Fig. 1E).

~~**Figure 2. Saint Agatha storm hydrodynamic data including significant wave height, Hs (m), wave period (s), and direction of wave approach (nautical degrees) and total water level (m) inclusive of barometric pressure effects, tide, and storm surge. The start and end time of the storm is referenced to the local storm threshold condition of Hs = 1.5 m and referenced to GMT.**~~

4 Methods

4.1 Quick Response Impact Assessment

~~The authors have developed and~~ present here a coordinated Quick Response Protocol (QRP) for a ~~quick~~ storm impact assessment to be implemented by Quick Response Team (QRT) by integrating EWS (Early Warning System) input, RTK GPS and drone survey techniques, along with quantitative observation and collection of data through interviews with local stakeholders and damage annotation. In the framework of the risk management cycle, the QRP is shown in Fig. 3. The available regional EWS is able to provide early information on the specific coastal areas within the regional domain that are likely to be

Nat. Hazards Earth Syst. Sci. Discuss., https://doi.org/10.5194/nhess-2017-337
Manuscript under review for journal Nat. Hazards Earth Syst. Sci.
Discussion started: 10 October 2017
© Author(s) 2017. CC BY 4.0 License.

Natural Hazards and Earth System Sciences
Discussions

impacted by an approaching storm. In this case study, the EWS has been operational for several years and is utilized by the Emilia-Romagna regional authority and results made available to the general community (http://geo.regione.emilia-romagna.it/schede/ews/). Thus, the QRT is able to know in advance where the protocol will most likely be needed and prepare in advance for personnel scheduling and survey equipment readiness. The pre-storm survey, mainly topo-bathymetric survey through both RTK GPS and drone techniques, should be performed whenever possible, given enough time and resources. ~~However, it is most critically necessary (i) in case studies where important morphological changes take place over short time-scales or (ii) when other sources of information are not available on the pre-storm condition in the likely impacted area~~. In this study, a pre-storm (October 2014) Lidar derived Digital Terrain Model (DTM) was used as reference for the pre-storm scenario. Moreover, the EWS can provide further guidance to the QRT by indicating when storm conditions have subsided sufficiently to allow survey activities on the ground and in the air.

The QRP for storm impact assessment included a sequence of steps to acquire both qualitative and quantitative measurements of the storm in the immediate aftermath of the event. The critical tasks of the quick response strategy during the days immediately following the storm included the following activities:

- Conduct interviews of citizens, shopkeepers, restaurant owners, and other local stakeholders;
- Annotate the visible damage to coastal defenses, buildings, infrastructures;
- Take pictures of the horizontal flood limits and vertical flood marks;
- Quantitatively measure the vertical elevation of flood marks on buildings and defense structures;
- Map the horizontal flood limit by means of RTK GPS;
- Survey of the beach by means of RTK GPS (profiles) and aerial drone flights.

The QRP steps provided data ~~to allow~~ for an integrated analysis of the storm impacts. The need to conduct rapid field survey activities in this study required the contribution of several people: at least 2 to 3 skilled operators were necessary to accomplish all the tasks in the field, every day. Depending on the alongshore extent and width of the coast that needs to be covered, the implementation of the protocol could last from a few days to a few weeks. In this study, 7 days were sufficient to complete the aforementioned tasks along a total beach extent of almost 7 km for the case study site (Fig. 1D), resulting in the integrated assessment rate of 1km per day. In total, 10 profiles and more than 40 flood limits and flood marks were surveyed with RTK GPS technique and 6km of beach were surveyed with the drone and a further 50-60 GCPs (Ground Control Points) were surveyed on the ground with RTK GPS for use in the drone data processing, error analysis and data comparison.

The data processing and analysis of the acquired information is further described in the next sections, specifically focusing on the target area (Fig. 1E). With regards to the stakeholder interviews, in this study, these were used mainly to understand which local areas were mostly impacted, in order to better organize the field activities, and to understand the timing of the storm impact evolution.

Nat. Hazards Earth Syst. Sci. Discuss., https://doi.org/10.5194/nhess-2017-337
Manuscript under review for journal Nat. Hazards Earth Syst. Sci.
Discussion started: 10 October 2017
© Author(s) 2017. CC BY 4.0 License.

Natural Hazards and Earth System Sciences Discussions

The integrated information will help to understand the overall impact of the storm in the surveyed area. The scientific aims of the QRP can also provide useful input to the coastal managers for hazard and risk assessment purposes (Fig. 3).

Figure 3. The Quick Response Protocol (QRP) in the framework of the Disaster Management Cycle.

~~**4.2 Pre-storm Conditions**~~

~~The pre-storm conditions of the subaerial beach and backshore were assumed to be represented by the available LIDAR-derived DTM from October 2014. The dataset was used as reference for the morphological variations of the emerged beach due to the storm impact, as no major events occurred in the period before the survey and the Saint Agatha event.~~

4.3 Ground GPS survey

Field measurements relative to flood limits, flood marks, and beach profiles were undertaken using a RTK GPS (Trimble R6). All measurements were referenced to WGS84 UTM33N coordinates and the national geoid Italgeo99 for elevation. The flood limit denotes the maximum water progression on the plan view, evidenced by the presence of objects and debris moved inland by the water during the storm, hereafter called "GPS Floodlines" in the study (Fig. 4A). A flood mark denotes the maximum water depth at a specific location where the water level was clearly visible, for example, walls, buildings, trees or dunes (Fig. 4B). These points, hereafter called "GPS Floodmarks", are associated with a GPS location and an observed water depth. Cross-shore beach profiles were also surveyed in order to have a comparison with the post-storm Digital Elevation Model (DEM) generated from the drone photogrammetry analysis. Ten cross-shore profiles were measured throughout the surveyed area highlighted in Fig. 1D. The profiles belonging to the case study target area are two (Profile 1 and Profile 2 in Fig. 1E). These profiles were then used to provide a validation/quantification of error of the drone processed data.

~~**Figure 4. Examples of "GPS Floodline" (A) and "GPS Floodmark" (B) measurements.**~~

4.4 Drone Survey and Ground Control Points

A commercial off-the-shelf unmanned aerial vehicle (UAV), the DJI Phantom Vision 2+, was used to conduct the aerial remote sensing imagery capture. Photos were collected from elevations between 40-60 m at speeds of 4 m/s with manual flight controls used to fly in a lawn-mower pattern (e.g. boustrophedon flight pattern) back and forth across the beach with 65-75% overlap between images resulting in more than five photos per common point within the survey domain. The drone camera utilized a fixed focal length, constant exposure, and timed image capture every five seconds. Fourteen Ground Control Points (GCPs) were taken using a RTK GPS (Trimble R6) for ~~use in correcting the UAV digital elevation model~~. A commercially available photogrammetry software package, specifically Pix4D, was used to stitch the collected UAV photos into one continuous mosaic by matching points within overlapping photos utilizing structure-from-motion (SfM) algorithms. The application of drone based SfM photogrammetry for coastal morphology assessment has been demonstrated recently by the studies of Casella et al., (2014; 2016), Turner et al., (2016), Dohner et al., (2016) and Scarelli et al. (2017). Drone photo post-processing followed the step-wise process illustrated in Fig. 5, whereby photos are matched using embedded GPS metadata from the UAV then

Nat. Hazards Earth Syst. Sci. Discuss., https://doi.org/10.5194/nhess-2017-337
Manuscript under review for journal Nat. Hazards Earth Syst. Sci.
Discussion started: 10 October 2017
© Author(s) 2017. CC BY 4.0 License.

Natural Hazards and Earth System Sciences
Discussions

GCPs are added to ~~the mosaic to constrain error with the more accurate RTK GPS positioning for horizontal and vertical control~~. Orthophoto mosaics are then reduced to dense points clouds with elevation values calculated from the stitched mosaic. Digital Elevation Models (DEMs) and mesh models are created from the dense point cloud. The DEM and orthomosaic were then exported for use in comparison to the RTK GPS survey (see Section 5). The drone based survey approach allowed to ~~quickly~~ survey an area of 0.25 km^2 within a 10-minute flight resulting in a ground sampling distance of 2.5 cm/pixel.

Figure 5. Sequence of processing steps used in the analysis of UAV photos to generate data output products.

5 Results

With the goal of demonstrating the reliability of an integrated assessment of the storm impacts, implemented following the QRP, the results of the extensive on-ground survey effort during the week following the storm are presented for the target area (Fig. 1E) of the pilot case study (Fig. 1D). The results are presented in sequential sections showing comparisons between the ~~on-the-ground (~~RTK-GPS~~)~~ and ~~aerial drone survey results~~.

5.1 Topographic Profiles and Digital Elevation Model Surface

An indication of the reliability of the DEM produced from the analysis of the drone images is given comparing it with the RTK GPS cross-section points (see Fig. 1E). The comparison is shown in Fig. 6 for both profiles. For both datasets the assumed vertical uncertainty is shown, namely ±15 cm for drone derived data and ±5 cm for RTK GPS data, illustrated by the shaded outlines. It is important to note that elevation outliers were deleted from the drone derived data extracted for Profile 1 and 2 when they were visually determined to be clearly not representative of the terrain surface. A smoothing of the profiles (drone and RTK GPS derived) was also applied. The Root Mean Square Errors (RMSEs) of the vertical elevation between the ground measured (RTK GPS) and remote sensing (drone) data were 14 cm and 12 cm for Profiles 1 and 2, respectively. Note that Profile 2, with an RMSE of 12 cm, is located in the central portion of the survey area, where more precision was expected due to greater image overlap and GCP control, while profile 1, with an RMSE of 14 cm, is closer to the edge of the domain where the drone DEM is expected to be less accurate. Since the drone data comes from a commercial off-the-shelf unit and thus relies on RTK GPS ground control points for positioning accuracy, the drone surveys are therefore not wholly independent of the GPS system. Nevertheless, the drone surveys provide a useful and efficient extension of the RTK GPS ground surveys. This target study aimed to give an indication of precision and reliability of the resulting drone DTM which was corrected using the available RTK GPS ground control points. The drone data, while overestimating the elevation in the higher portion of the Profile 1, with the strongest difference in the order of 25-30cm, converged with the RTK GPS profile in the lower portion of Profile 1 near the swash zone. For Profile 2, most of the morphological features were captured, including the storm berm (with a vertical error on the berm top of ~15cm). The slopes of the emerged foreshore are comparable for both profiles: for Profile 1 the slope calculated was 0.016 for the drone derived profile, while it resulted 0.014 for the RTK GPS profile. The same

© Author(s) 2017. CC BY 4.0 License.

slopes calculated for Profile 2 resulted 0.021 and 0.018, respectively. This profile convergence is implemented in further morphological change analysis as shown in Section 5.3.

Thus, the foreshore slope, berm shape, and berm crest locations are well captured by the drone DEM in Fig. 6. The largest disagreement between the drone and RTK GPS profiles occurs landward of the berm in the back portion of the beach (around 30cm for Profile 1 and 20cm for Profile 2). A combination of factors may have contributed to this difference including lower sampling resolution of the RTK GPS compared to the drone, higher uncertainties in the drone elevations, and inclusion of non-terrain elevations such as wood and debris in the DEM (see Section 6.1).

Figure 6. Comparisons between the February 2015 post-storm observed GPS profile survey and post-storm drone DEM for Profiles 1 and 2.

5.2 Coastal Flooding

In Fig. 7, the results obtained for the flood extent from the drone derived data are shown in comparison with the GPS observed Floodline and Floodmarks. The drone orthomosaic was analyzed to extract the floodline extent by observing the debris line that was deposited inland (i.e. "Drone Floodline" in Fig. 7). In order to also take into account visible areas in the drone orthomosaic that were reached by the water through small paths but that are not included in the main flooded area (defined as previously described in Section 4.4), several spot areas, hereby and in Fig. 7 called "Drone Secondary Flood" areas, were defined. ~~Notably, the high-resolution of the orthomosaic enabled to extract a really detailed continuous flood extent, if compared to the GPS survey.~~

An agreement is seen between the "Drone Floodline" and the RTK GPS derived flood line ("GPS Floodline"). As both depend on the observation of objects and debris moved inland during the storm that remained visible during both the GPS survey and in the drone orthomosaic, the comparison can be considered as validation of the drone orthomosaic for remote sensing of storm floodlines. The flooding was mainly limited to the ~~subaerial~~ beach in front of the concessions (Fig. 7). Some of the concessions, however, experienced an indirect flooding where the limit of the flood reached the border of the concessions and the water found a path to flow in to the properties (Fig. 7, A, B, C, D). A water depth of 30cm was measured in the location of the flood mark (Fig. 7, A).

~~**Figure 7. Observed "GPS Floodline" and "GPS Floodmark" (green and red circles), drone (red solid line and light-blue polygons) flood extent comparisons: the box on the left shows an overview of the target area while on the right (A, B, C and D) some spot-focuses are given.**~~

5.3 Erosion and Sedimentation Patterns

The erosion and sedimentation patterns are shown in Fig. 8. The drone derived patterns (Fig. 8, A1, B1 and C1) were obtained from the comparison between the DTM of October 2014 and the post-event DEM generated by the drone. The results are only presented for the area limited by the GCPs. Notably, as the drone derived DEM included non-terrain objects and buildings, the analysis of the morphological features only focused on the emerged beach. The inclusion of non-beach features in the drone derived DEM, mainly because of the presence of different sized debris, affected the non-uniformity of the drone derived pattern.

Nat. Hazards Earth Syst. Sci. Discuss., https://doi.org/10.5194/nhess-2017-337
Manuscript under review for journal Nat. Hazards Earth Syst. Sci.
Discussion started: 10 October 2017
© Author(s) 2017. CC BY 4.0 License.

Natural Hazards and Earth System Sciences
Discussions

The morphological features are recognizable in the drone orthomosaic (Fig. 8~~,~~ A). A general lowering of the backshore can be noted especially from the drone results (Fig. 8, A1), which ~~actually~~ corresponds to the area where the differences between the RTK GPS profiles and the drone derived one were higher (see Section 5.1 and Fig. 6). From the drone results (Fig. 8, A1) a formation of a storm berm is clearly visible running alongshore with a varying width of 20 to 50m. The vertical deposit is interrupted by erosion scour channels due to some return flows (Fig. 8, A1). Seaward the depositional area (i.e. the berm) an erosion pattern highlights a trough formation, which emphasizes just in front of the scour channels (Fig. 8, A1). Thus, the berm vertically grew and moved landward during the storm as result of motion of sediments in the breaker zone (Fig. 8, A1). At the same time, a small portion of deposit in the intertidal area corresponds to the development of the intertidal bar, just at the edge of the analyzed domain. Focusing on the selected frames (Fig. 8, B, B1, C, C1), visible scour channels are highlighted, that developed from the footpaths which provided the fastest preferential way for the water to flow back to sea during the storm. This highlights the UAV's ability to map fine~~r~~ resolution features such as scour channels.

~~**Figure 8. Morphological variations: (A) the drone orthomosaic of the target area, where morphological features are visible along with the position of the GCPs; (A1) the difference between the post-event drone-derived DEM and the pre-storm Lidar-derived DEM. In B, B1 and C, C1 enlargements of the main features are given. The morphological variations are only shown for the area surrounded by the GCPs.**~~

6 Discussion and Recommendations

~~In this section the authors discuss the results, along with their limitations, with focus on the comparisons between gps and drone derived data. Then, practical and general recommendations are given in order to provide possible ways to improve the QRP application and the quality of the data.~~

6.1 Discussion

The variability in vertical accuracy seen in the drone derived-data was mainly related to the flight parameters (manual flight, variable altitude and timed image capture), the number and type of GCPs used to constrain the DEM and SfM equations used in each software processing workflow. A recent study by James et al., (2017) provides practical suggestions for photogrammetric considerations (i.e. modifications to drone flight characteristics) control considerations (i.e. the number and spacing of GCPs) that echo the operational findings from our study, namely that overall DEM improvement is achieved through increased numbers of overlapping imagery and greater number of distributed GCPs. Of note with regards to our DEM analysis, non-terrain objects (i.e. human structures and debris) were not removed from the point cloud during processing and remained in the resulting DEM as was seen also in a similar storm response study by Casella et al., (2014). Thus, objects such as wood, litter and buildings, locally affected the represented surface and, consequently, the comparison with the post-storm RTK GPS observations and the pre-storm DTM data, which only represented the terrain surface. Notably, the profile comparisons show disturbances that can be due to these aspects. Also, the drone derived DEM should be considered valid in the area limited by the GCPs. The RMSEs of 14 cm and 12 cm vertically, that were calculated between the drone processed DEM ~~from photogrammetry processing using GCPs and the RTK GPS data~~ (Fig. 6), are similar for both analyzed profiles and comparable

© Author(s) 2017. CC BY 4.0 License.

with the Lidar derived data uncertainty. In comparison with error estimates of drone products reported by recent studies, the resulting RMSE values of the drone DEM compared to the traditional RTK GPS profile surveys are comparable (Casella, 2014 & 2016; Dohner et al., 2016) or higher (Turner et al., 2016; James et al., 2017; Scarelli et al., 2017). This is attributed to manual flights and inappropriate GCP selections which were unidentifiable due to image resolution at the survey altitude. However, the resulting drone DEM was still able to well capture morphological features.

The drone derived orthomosaic offered ~~a very easy and quick~~ way to ~~assess~~ the flood extent ~~of the event~~. The general agreement with the RTK GPS on the ground observations confirmed the close geopositioning of the images and provided a validation of the assessed flood extent. Notably, the opportunity to observe the flooding extent from the drone data made it possible to define a really detailed and continuous floodline. In order to obtain the same results with a GPS survey, the operator should increase the point sampling (or even use a continuous sampling method). This implies prolonging the field activities on the beach. Also, the drone point of view is essential to have a complete view of the flood line evolution while, from the GPS point of view, the random distribution and spreading of the debris can mislead the operator.

The morphological patterns derived from the drone data gave an opportunity to assess the morphological response of the beach at a very detailed resolution. From a geomorphologic point of view, the formation of an intertidal bar after a storm event was also noticed by Armaroli et al., ~~2013~~. The scouring channels highlighted in Fig. 8 were triggered by the presence of concrete pathways of local activities that concentrated and accelerated the return water flux during the storm. In order to reduce the formation of these scouring channels and the consequent worsening of beach erosion, a reasonable choice would be to remove, or at least retreat landward, the pathways during the winter season (Nordstrom et al., 2015).

6.2 Practical Recommendations

Through the initial rapid response field collection effort the research team determined specific methodologies to ensure quality data following a major storm event. With respect to remote sensing drone survey, the placement and quantity of GCPs, plays a critical role in the resulting DEM and its uncertainty. In order to obtain vertical and horizontal errors shown in Fig. 9, the following guidelines are suggested for flight planning and GCP distribution:

- Perform drone flight surveys at the same altitude and image overlap. This is easily done with an autopilot and mission planning application available to phones and tablets.
- Survey a significantly larger domain (~10% buffer) than needed for data collection. Survey domain edge photos are often removed due to low overlap between images and data is lost.
- Distribute GCPs throughout survey domain and near boundaries to prevent skewing within the DEM.
- GCPs should be flat, large, and uniquely shaped or marked in such a manner as to be confidently identified from aerial images.

© Author(s) 2017. CC BY 4.0 License.

- On the ground photos of GCP locations should be taken to give a concept of exactly where the RTK GPS point were taken on the target object and within the context of the survey domain.
- Remove outlier and/or non-terrestrial points from the dense point cloud such as storm debris, people, and vehicles for surface calculations

A visual representation of the bulleted list is presented in Fig. 9 with images of positive (9A and 9B) and poor (9C and 9D) quality GCPs.

Qualitative observations and interviews are also important and should be performed as soon as possible and as detailed as possible during the implementation of the QRP. Thus, the larger is the number of people involved for the post-event survey, the fastest can be the collection of data as the team can be divide in thematic groups. Planning the activities is crucial for the good performance of the team. This can be additionally supported by activities performed during the non-storm season, such as instrument maintenance and preparation, monitoring of the EWS performances, tasks planning and assignment, etc.

~~**Figure 9. Photos A and B at the top demonstrate practical GCPs based on unique shapes, colors, and ability to see from a high altitude. Photos C and D, on the bottom, demonstrate error-inducing GCPs due to their height off the ground and indistinguishable shape, size, and color in aerial images.**~~

6.3 General Recommendations

In order to provide more accurate qualitative outcomes further analyses should be performed. This paper only presents the analysis of a small portion (Fig. 1E) of the whole case study (Fig. 1D) and deeper investigations are needed to provide more robust outcomes. However, the QRP has been demonstrated to be a proper approach to quickly assess the storm impacts along the coast in the immediate aftermath of an event, as a combination of technologies and planning approaches. Thus, in the framework of coastal management (Fig. 3), a proper application of the protocol can produce useful information that can be used at local, regional and national levels in order to, as example: (i) update hazard and risk maps; (ii) provide detailed information for flood-damage curves calibration (see, as example, the study of Scorzini and Frank, 2015); (iii) provide insights for risk mitigation and management plans.

7 Conclusions

This study illustrates the potentialities of an integrated approach combining aerial drones together with on the ground RTK GPS surveys and qualitative data collection for coastal storm impact assessments at local level. The presented protocol was applied at a pilot case study in the Emilia-Romagna coast and results were presented and discussed, for demonstration purposes, on a small portion of the pilot case study. Limitations of the application were highlighted and recommendations for improvements were given. As general remark, the drone approach was found to be effective for flooding and erosion impact assessments, being able to provide detailed, continuous and two-dimensional information, with a limited time effort on the

© Author(s) 2017. CC BY 4.0 License.

field in comparison with the traditional GPS methodologies. Notably, further applications of the approach can directly support hazard and risk assessment efforts at local and regional level (e.g., hazard and risk maps updating, calibration of flood-damage curves, etc.), and thus addressing coastal management needs.

Competing interests

The authors declare that they have no conflict of interest.

Acknowledgements

The work was facilitated by a sabbatical grant to A. Trembanis and ongoing programmatic support to P. Ciavola by the European Community's 7th Framework Programme through the grant to RISC-KIT ("Resilience-increasing Strategies for Coasts – Toolkit"), contract no. 603458. Acquisition and utilization of the UAV system was made possible through funding from the UNIDEL foundation and from NOAA Sea Grant project NOAA SG-2016-18 RRCE-8 TREMBANIS. The authors are also thankful to Drs. Clara Armaroli, Duccio Bertoni, Mohammad Muslim Uddin, and Sarah Trembanis for their help on gathering data on the field.

References

Anderson, K. and Gaston, K. J.: Lightweight unmanned aerial vehicles will revolutionize spatial ecology, Front. Ecol. Environ., 11(3), 138–146, 2013.

Armaroli, C. and Duo, E.: Validation of the Coastal Storm Risk Assessment Framework along the Emilia-Romagna coast, Coast. Eng., (RISC-KIT Special Issue), doi:10.1016/j.coastaleng.2017.08.014, 2017.

Armaroli, C., Ciavola, P., Masina, M. and Perini, L.: Run-up computation behind emerged breakwaters for marine storm risk assessment, J. Coast. Res., SI 56, 1612–1616, 2009.

Armaroli, C., Ciavola, P., Perini, L., Calabrese, L., Lorito, S., Valentini, A. and Masina, M.: Critical storm thresholds for significant morphological changes and damage along the Emilia-Romagna coastline, Italy, Geomorphology, 143–144, 34–51, doi:10.1016/j.geomorph.2011.09.006, 2012.

© Author(s) 2017. CC BY 4.0 License.

Armaroli, C., Grottoli, E., Harley, M. D. and Ciavola, P.: Beach morphodynamics and types of foredune erosion generated by storms along the Emilia-Romagna coastline, Italy, Geomorphology, 199, 22–35, doi:10.1016/j.geomorph.2013.04.034, 2013.

Arpa Emilia-Romagna: Rapporto dell'evento meteorologico del 5 e 6 febbraio 2015, Bologna. [online] Available from: http://www.arpa.emr.it/cms3/documenti/_cerca_doc/meteo/radar/rapporti/Rapporto_meteo_20150205-06.pdf, 2015.

Bason, C., Jacobs, A., Howard, A. and Tymes, M.: White Paper on the Status of Sudden Wetland Dieback in Saltmarshes of the Delaware Inland Bays, Delaware Department of Natural Resources & Environmental Control., 2007.

Benedet, L., Finkle, C. W. and Hartog, W. M.: Processes controlling development of erosional hot spots on a beach nourishment project, J. Coast. Res., 23(1), 33–48, 2007.

Berni, J. A. J., Zarco-Tejada, P. J., Suarez, L. and Fereres, E.: Thermal and narrowband multispectral remote sensing for vegetation monitoring from an unmanned aerial vehicle, IEEE Trans. Geosci. Remote Sens., 47(3), 722–738, 2009.

Bernstein, D. J., Freeman, C., Forte, M. F., Park, J. Y., Gayes, P. T. and Mitasova, H.: Survey design analysis for three-dimensional mapping of beach and nearshore morphology, in Proceedings of the Coastal Sediment '03, St. Petersburg, Florida, USA., 2003.

Billi, P. and Rinaldi, M.: Human impact on sediment yield and channel dynamics in the Arno River basin (central Italy), in Human Impact on Erosion and Sedimentation (Proceedings of Rabat Symposium S6, April 1997), pp. 301–311, IAHS Press, Institute of Hydrology, Wallingford, Oxfordshire, UK., 1997.

© Author(s) 2017. CC BY 4.0 License.

Bush, D. M., Neal, W. J., Young, R. S. and Pilkey, O. H.: Utilization of geoindicators for rapid assessment of coastal-hazard risk and mitigation, Ocean Coast. Manag., 42, 647–670, doi:10.1016/S0964-5691(99)00027-7, 1999.

Casella, E., Rovere, A., Pedroncini, A., Mucerino, L., Casella, M., Cusati, L. A., Vacchi, M., Ferrari, M. and Firpo, M.: Study of wave runup using numerical models and low-altitude aerial photogrammetry: A tool for coastal management, Estuar. Coast. Shelf Sci., 149, 160–167, doi:10.1016/j.ecss.2014.08.012, 2014.

Casella, E., Rovere, A., Pedroncini, A., Stark, C. P., Casella, M., Ferrari, M. and Firpo, M.: Drones as tools for monitoring beach topography changes in the Ligurian Sea (NW Mediterranean), Geo-Marine Lett., 1–13, doi:10.1007/s00367-016-0435-9, 2016.

Ciavola, P., Ferreira, O., Haerens, P., Van Koningsveld, M. and Armaroli, C.: Storm impacts along European coastlines. Part 2: Lessons learned from the MICORE project, Environ. Sci. Policy, 14(7), 924–933, doi:10.1016/j.envsci.2011.05.009, 2011.

Dohner, S. M., Trembanis, A. C. and Miller, D. C.: A tale of three storms: Morphologic response of Broadkill Beach, Delaware, following Superstorm Sandy, Hurricane Joaquin, and Winter Storm Jonas, Shore & Beach, 84(4), 2016.

Van Dongeren, A., Ciavola, P., Martinez, G., Viavattene, C., Bogaard, T., Ferreira, Ó., Higgins, R. and McCall, R.: Introduction to RISC-KIT: Resilience-increasing strategies for coasts, Coast. Eng., (RISC-KIT Special Issue), in review, n.d.

Hansen, J. E. and Barnard, P. L.: Sub-weekly to interannual variability of a high-energy shoreline, Coast. Eng., 57, 959–972, 2010.

© Author(s) 2017. CC BY 4.0 License.

Harley, M. D., Valentini, A., Armaroli, C., Ciavola, P., Perini, L., Calabrese, L. and Marucci, F.: An early warning system for the on-line prediction of coastal storm risk on the Italian coastline, in Coastal Engineering 2012. [online] Available from: http://new.every1graduates.org/wp-content/uploads/2012/03/Early_Warning_System_Neild_Balfanz_Herzog.pdf%5Cnhttp://journals.tdl.org/icce/index.php/icce/article/view/6702, 2012.

Harley, M. D., Valentini, A., Armaroli, C., Perini, L., Calabrese, L. and Ciavola, P.: Can an early-warning system help minimize the impacts of coastal storms? A case study of the 2012 Halloween storm, northern Italy, Nat. Hazards Earth Syst. Sci., 16(1), 209–222, doi:10.5194/nhess-16-209-2016, 2016.

James, M. R., Robson, S. and Smith, M. W.: 3-D uncertainty-based topographic change detection with structure-from-motion photogrammetry: precision maps for ground control and directly georeferenced surveys, Earth Surf. Process. Landforms, doi:10.1002/esp.4125, 2017.

Larson, M. and Kraus, N. C.: Temporal and spatial scales of beach profile change, Duck, North Carolina, Mar. Geol., 117, 75–94, 1994.

Lee, G.-H., Nicholls, R. J. and Birkhemeier, W. A.: Storm-driven variability of the beach-nearshore profile at Duck, North Carolina, USA, 1981-1991, Mar. Geol., 148, 163–177, 1998.

Lee, J. M., Park, J. Y. and Choi, J. Y.: Evaluation of sub-aerial topo- graphic surveying techniques using total station and RTK- GPS for applications in macrotidal sand beach environment, J. Coast. Res., 1(SI 65), 535–540, doi:10.2112/SI65-091.1, 2013.

Mancini, F., Dubbini, M., Gattelli, M., Stecchi, F., Fabbri, S. and Gabbianelli, G.: Using unmanned aerial vehicles (UAV) for high-resolution reconstruction of topography: The structure from motion approach on coastal environments, Remote Sens., 5(12), 6880–6898, doi:10.3390/rs5126880, 2013.

© Author(s) 2017. CC BY 4.0 License.

Masina, M. and Ciavola, P.: Analisi dei livelli marini estremi e delle acque alte lungo il litorale ravennate, Stud. costieri, 18, 87–101, 2011.

Mendoza, E. T. and Jimenez, J. A.: Storm-Induced Beach Erosion Potential on the Catalonian Coast, J. Coast. Res., Special Is(48), 81–88, 2006.

Mendoza, E. T., Jimenez, J. A. and Mateo, J.: A coastal storms intensity scale for the Catalan sea (NW Mediterranean), Nat. Hazards Earth Syst. Sci., 11(9), 2453–2462, doi:10.5194/nhess-11-2453-2011, 2011.

Morton, R. A.: Factors Controlling Storm Impacts on Coastal Barriers and Beaches-A Preliminary Basis for, J. Coast. Res., 18(3), 486–501, 2002.

Morton, R. A., Leach, M. P., Paine, J. G. and Cardonza, M. A.: Monitoring beach changes using GPS surveying techniques, J. Coast. Res., 9(3), 702–720, 1993.

Nicholls, R. J., Wong, P. P., Burkett, V. R., Codignotto, J. O., Hay, J. E., McLean, R. F., Ragoonaden, S. and Woodroffe, C. D.: Coastal systems and low-lying areas. Climate Change 2007: Impacts, Adaptation and Vulnerability. Contribution of Working Group II to the Fourth Assessment Report of the Intergovernmental Panel on Climate Change., Cambridge University Press, Cambridge, Massachussets., 2007.

Nordstrom, K. F., Armaroli, C., Jackson, N. L. and Ciavola, P.: Opportunities and constraints for managed retreat on exposed sandy shores: Examples from Emilia-Romagna, Italy, Ocean Coast. Manag., 104, 11–21, doi:10.1016/j.ocecoaman.2014.11.010, 2015.

Perini, L., Luciani, P. and Calabrese, L.: Altimetria della fascia costiera, in Il sistema mare-costa dell'Emilia-Romagna, edited by L. Perini and L. Calabrese, pp. 57–66, Regione Emilia-Romagna, Bologna, Italy., 2010.

Perini, L., Calabrese, L., Lorito, S. and Luciani, P.: Costal flood risk in Emilia-Romagna (Italy): the sea storm of

© Author(s) 2017. CC BY 4.0 License.

February 2015, in Coastal and Maritime Mediterranean Conference, EDITION 3, FERRARA, ITALY (2015), pp. 225–230., 2015a.

Perini, L., Calabrese, L., Lorito, S. and Luciani, P.: Il rischio da mareggiata in Emilia-Romagna : l ' evento del 5-6 Febbraio 2015, Geol., 53, 8–17 [online] Available from: http://www.geologiemiliaromagna.it/il-geologo-anno-xv-2015-n-53/, 2015b.

Perini, L., Calabrese, L., Salerno, G., Ciavola, P. and Armaroli, C.: Evaluation of coastal vulnerability to flooding: comparison of two different methodologies adopted by the Emilia-Romagna region (Italy), Nat. Hazards Earth Syst. Sci., 16(1), 181–194, doi:10.5194/nhess-16-181-2016, 2016.

Pietro, L. S., O'Neal, M. A. and Puleo, J. A.: Developing terrestrial-LIDAR-based digital elevation models for monitoring beach nourishment performance, J. Coast. Res., 24(6), 1555–1564, 2008.

Preciso, E., Salemi, E. and Billi, P.: Land use changes, torrent control works and sediment mining: Effects on channel morphology and sediment flux, case study of the Reno River (Northern Italy), Hydrol. Process., 26(8), 1134–1148, doi:10.1002/hyp.8202, 2012.

Saye, S. E., Van der Wal, D., Pye, K. and Blott, S. J.: Beach–dune morphological relationships and erosion/accretion: an investigation at five sites in England and Wales using LIDAR data, Geomorphology, 72(1), 128–155, 2005.

Scarelli, F. M., Sistilli, F., Fabbri, S., Cantelli, L., Barboza, E. G. and Gabbianelli, G.: Seasonal dune and beach monitoring using photogrammetry from UAV surveys to apply in the ICZM on the Ravenna coast (Emilia-Romagna, Italy), Remote Sens. Appl. Soc. Environ., 7(June), 27–39, doi:10.1016/j.rsase.2017.06.003, 2017.

Scorzini, A. R. and Frank, E.: Flood damage curves: New insights from the 2010 flood in Veneto, Italy, J. Flood

© Author(s) 2017. CC BY 4.0 License.

Risk Manag., 1–12, doi:10.1111/jfr3.12163, 2015.

Stockdon, H. F., Sallenger, A.H., J., List, J. H. and Holman, R. A.: Estimation of shoreline position and change using airborne topographic LIDAR data, J. Coast. Res., 18(3), 502–513, 2002.

Stone, G. W., Liu, B., Pepper, D. A. and Wang, P.: The importance of extratropical and tropical cyclones on the shore-term evolution of barrier islands along the northern Gulf of Mexico, USA, Mar. Geol., 210, 63–78, 2004.

Swales, A.: Geostatistical estimation of short-term changes in beach morphology and sand budget, J. Coast. Res., 18(2), 338–351, 2002.

Sytnik, O. and Stecchi, F.: Disappearing coastal dunes: tourism development and future challenges, a case-study from Ravenna, Italy, J. Coast. Conserv., 19(5), 715–727, doi:10.1007/s11852-014-0353-9, 2014.

Taramelli, A., Di Matteo, L., Ciavola, P., Guadagnano, F. and Tolomei, C.: Temporal evolution of patterns and processes related to subsidence of the coastal area surrounding the Bevano River mouth (Northern Adriatic) - Italy, Ocean Coast. Manag., 108, 74–88, doi:10.1016/j.ocecoaman.2014.06.021, 2015.

Teatini, P., Ferronato, M., Gambolati, G., Bertoni, W. and Gonella, M.: A century of land subsidence in Ravenna, Italy, Environ. Geol., 47(6), 831–846, doi:10.1007/s00254-004-1215-9, 2005.

Theuerkauf, E. J. and Rodriguez, A. B.: Impacts of transect location and variations in along-beach morphology on measuring volume change, J. Coast. Res., 28(3), 707–718, 2012.

Trembanis, A., Duval, C., Beaudoin, J. and Schmidt, V.: A detailed seabed signature from Hurricane Sandy revealed in bedforms and scour, , 14(10), 4334–4340, doi:10.1002/ggge.20260, 2013.

Turner, I. L., Harley, M. D. and Drummond, C. D.: UAVs for coastal surveying, Coast. Eng., 114, 19–24, doi:10.1016/j.coastaleng.2016.03.011, 2016.

© Author(s) 2017. CC BY 4.0 License.

Viavattene, C., Jiménez, J. A., Ferreira, O., Priest, S., Owen, D. and McCall, R.: Selecting coastal hotspots at the regional scale: the Coastal Risk Assessment Framework, Coast. Eng., in review, n.d.

Westoby, M. J., Brasington, J., Glasser, N. F., Hambrey, M. J. and Reynolds, J. M.: "Structure-from-Motion" photogrammetry: A low-cost, effective tool for geoscience applications, Geomorphology, 179, 300–314, 2012.

Young, A. P. and Ashford, S. A.: Performance evaluation of seacliff erosion control methods, Shore & Beach, 74(4), 16, 2006.

© Author(s) 2017. CC BY 4.0 License.

Figure 1. Field study site locations: A) Emilia-Romagna region; B) Coastal regional domain; C) Locations of the nearest tide gauge and wave buoy; D) Pilot case study site; E) Target area for data comparison.

Figure 2. Saint Agatha storm hydrodynamic data including significant wave height, Hs (m), wave period (s), and direction of wave approach (nautical degrees) and total water level (m) inclusive of barometric pressure effects, tide, and storm surge. The start and end time of the storm is referenced to the local storm threshold condition of Hs = 1.5 m and referenced to GMT.

Figure 3. The Quick Response Protocol (QRP) in the framework of the Disaster Management Cycle.

Figure 4. Examples of "GPS Floodline" (A) and "GPS Floodmark" (B) measurements.

Figure 5. Sequence of processing steps used in the analysis of UAV photos to generate data output products.

Figure 6. Comparisons between the February 2015 post-storm observed GPS profile survey and post-storm drone DEM for Profiles 1 and 2.

Figure 7. Observed "GPS Floodline" and "GPS Floodmark" (green and red circles), drone (red solid line and light-blue polygons) flood extent comparisons: the box on the left shows an overview of the target area while on the right (A, B, C and D) some spot-focuses are given.

Figure 8. Morphological variations: (A) the drone orthomosaic of the target area, where morphological features are visible along with the position of the GCPs; (A1) the difference between the post-event drone-derived DEM and the pre-storm Lidar-derived DEM. In B, B1 and C, C1 enlargements of the main features are given. The morphological variations are only shown for the area surrounded by the GCPs.

Figure 9. Photos A and B at the top demonstrate practical GCPs based on unique shapes, colors, and ability to see from a high altitude. Photos C and D, on the bottom, demonstrate error-inducing GCPs due to their height off the ground and indistinguishable shape, size, and color in aerial images.

Nat. Hazards Earth Syst. Sci. Discuss., https://doi.org/10.5194/nhess-2017-337
Manuscript under review for journal Nat. Hazards Earth Syst. Sci.
Discussion started: 10 October 2017
© Author(s) 2017. CC BY 4.0 License.

Natural Hazards and Earth System Sciences
Discussions

Fig. 1.

Nat. Hazards Earth Syst. Sci. Discuss., https://doi.org/10.5194/nhess-2017-337
Manuscript under review for journal Nat. Hazards Earth Syst. Sci.
Discussion started: 10 October 2017
© Author(s) 2017. CC BY 4.0 License.

Natural Hazards and Earth System Sciences
Discussions

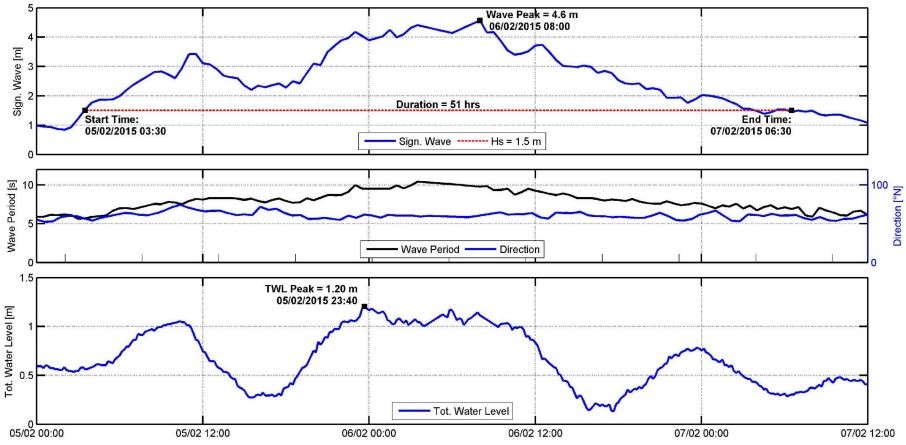

Fig. 2.

Nat. Hazards Earth Syst. Sci. Discuss., https://doi.org/10.5194/nhess-2017-337
Manuscript under review for journal Nat. Hazards Earth Syst. Sci.
Discussion started: 10 October 2017
© Author(s) 2017. CC BY 4.0 License.

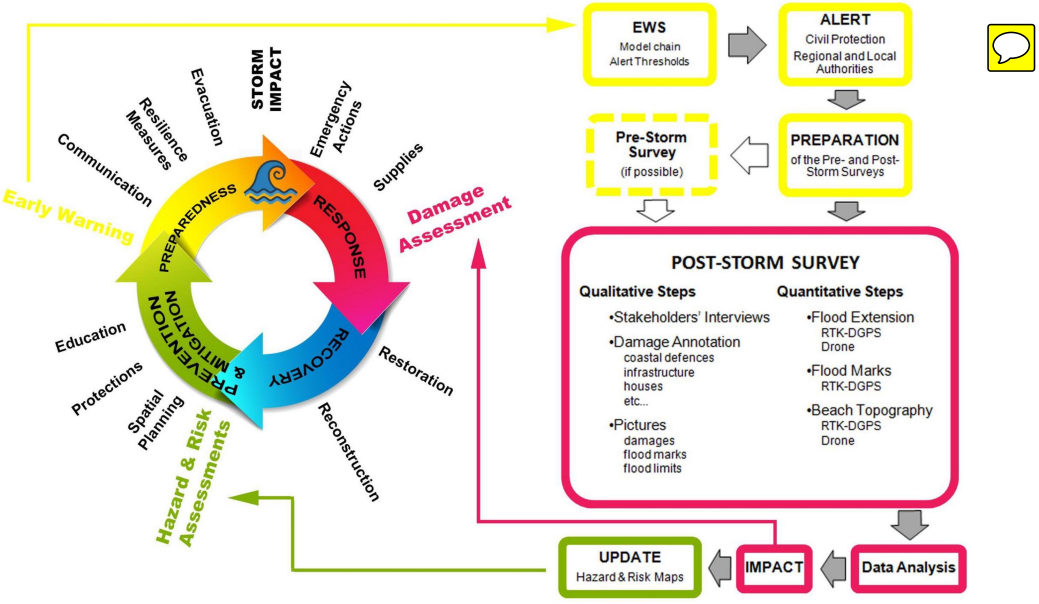

Fig. 3.

Nat. Hazards Earth Syst. Sci. Discuss., https://doi.org/10.5194/nhess-2017-337
Manuscript under review for journal Nat. Hazards Earth Syst. Sci.
Discussion started: 10 October 2017
© Author(s) 2017. CC BY 4.0 License.

Natural Hazards and Earth System Sciences
Discussions

Fig. 4.

Nat. Hazards Earth Syst. Sci. Discuss., https://doi.org/10.5194/nhess-2017-337
Manuscript under review for journal Nat. Hazards Earth Syst. Sci.
Discussion started: 10 October 2017
© Author(s) 2017. CC BY 4.0 License.

Natural Hazards and Earth System Sciences
Discussions

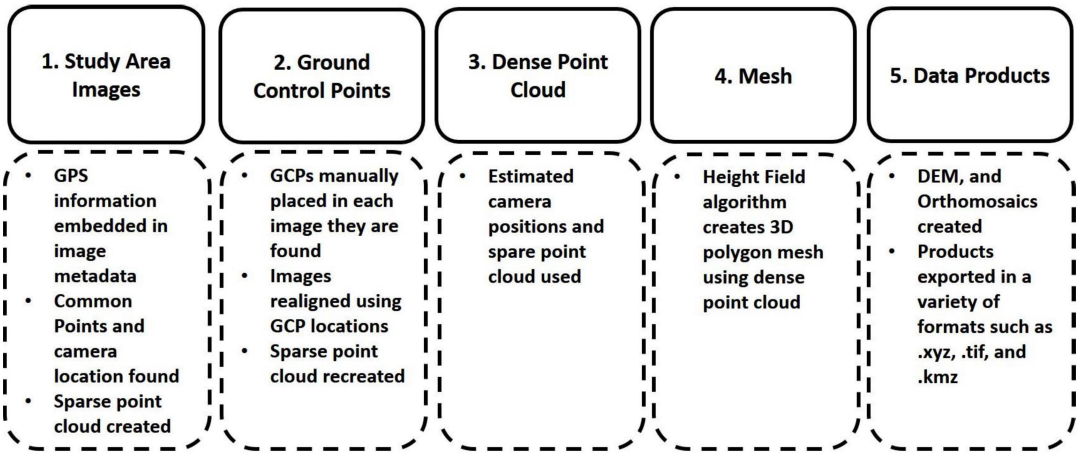

Fig. 5.

Nat. Hazards Earth Syst. Sci. Discuss., https://doi.org/10.5194/nhess-2017-337
Manuscript under review for journal Nat. Hazards Earth Syst. Sci.
Discussion started: 10 October 2017
© Author(s) 2017. CC BY 4.0 License.

Natural Hazards and Earth System Sciences
Discussions
Open Access
EGU

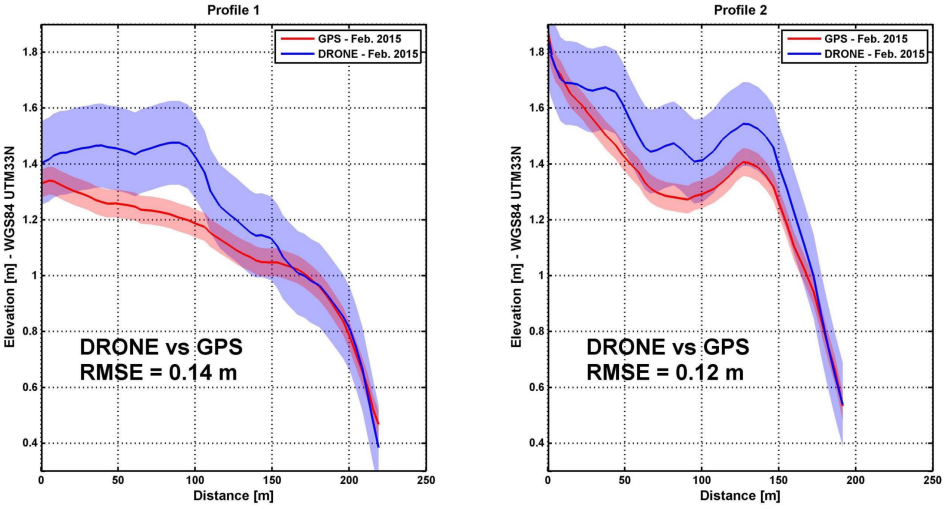

Fig. 6.

Nat. Hazards Earth Syst. Sci. Discuss., https://doi.org/10.5194/nhess-2017-337
Manuscript under review for journal Nat. Hazards Earth Syst. Sci.
Discussion started: 10 October 2017
© Author(s) 2017. CC BY 4.0 License.

Natural Hazards and Earth System Sciences
Discussions

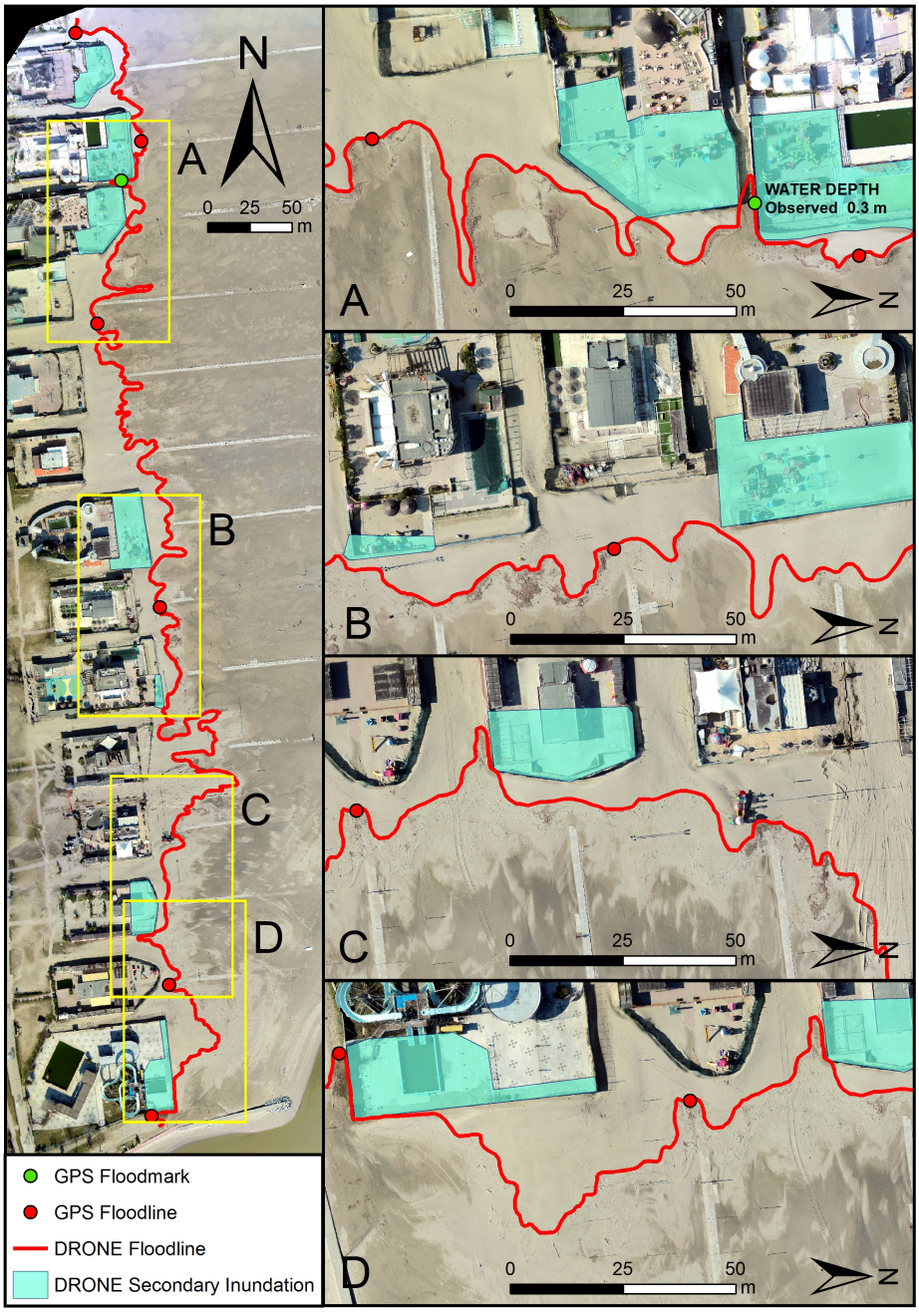

Fig. 7.

Nat. Hazards Earth Syst. Sci. Discuss., https://doi.org/10.5194/nhess-2017-337
Manuscript under review for journal Nat. Hazards Earth Syst. Sci.
Discussion started: 10 October 2017
© Author(s) 2017. CC BY 4.0 License.

Natural Hazards and Earth System Sciences
Discussions

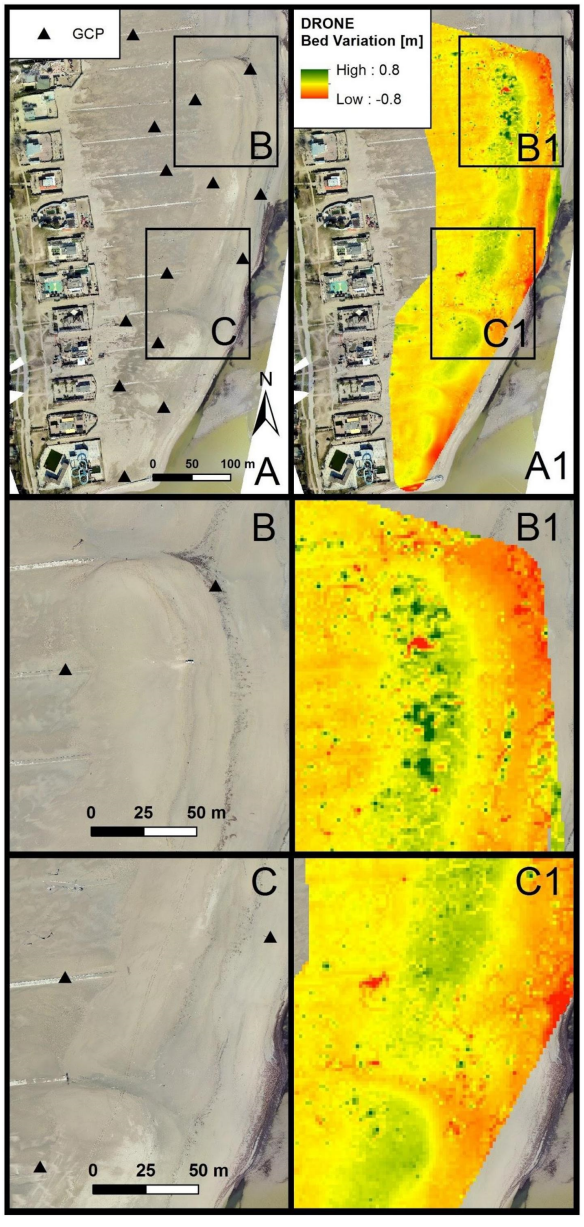

Fig. 8.

Nat. Hazards Earth Syst. Sci. Discuss., https://doi.org/10.5194/nhess-2017-337
Manuscript under review for journal Nat. Hazards Earth Syst. Sci.
Discussion started: 10 October 2017
© Author(s) 2017. CC BY 4.0 License.

Natural Hazards and Earth System Sciences
Discussions

Fig. 9.